Biochemistry

pubs.acs.org/biochemistry Article

Visualization of Platelet Integrins via Two-Photon Microscopy Using Anti-transmembrane Domain Peptides Containing a Blue Fluorescent Amino Acid

Karen P. Fong, Ismail A. Ahmed, Marco Mravic, Hyunil Jo, Oleg V. Kim, Rustem I. Litvinov, John W. Weisel, William F. DeGrado, Feng Gai, and Joel S. Bennett*

Cite This: *Biochemistry* 2021, 60, 1722−1730 Read Online

ACCESS | Metrics & More | Article Recommendations

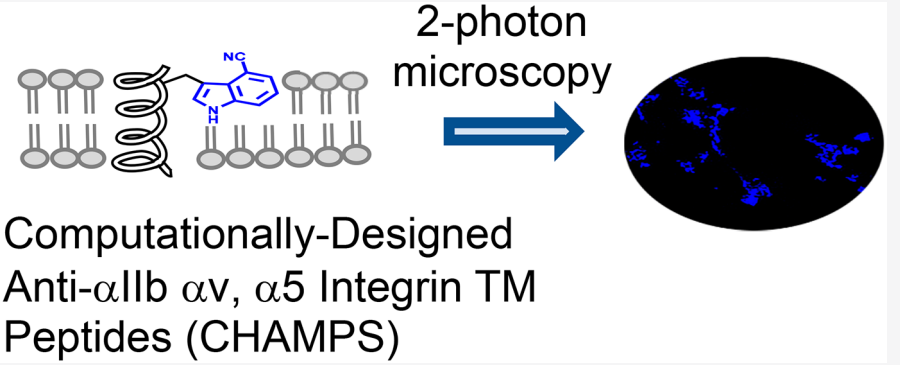

ABSTRACT: The fluorescent reporters commonly used to visualize proteins can perturb both protein structure and function. Recently, we found that 4-cyanotryptophan (4CN-Trp), a blue fluorescent amino acid, is suitable for one-photon imaging applications. Here, we demonstrate its utility in two-photon fluorescence microscopy by using it to image integrins on cell surfaces. Specifically, we used solid-phase peptide synthesis to generate CHAMP peptides labeled with 4-cyanoindole (4CNI) at their N-termini to image integrins on cell surfaces. CHAMP (computed helical anti-membrane protein) peptides spontaneously insert into membrane bilayers to target integrin transmembrane domains and cause integrin activation. We found that 4CNI labeling did not perturb the ability of CHAMP peptides to insert into membranes, bind to integrins, or cause integrin activation. We then used two-photon fluorescence microscopy to image 4CNI-containing integrins on the surface of platelets. Compared to a 4CNI-labeled scrambled peptide that uniformly decorated cell surfaces, 4CNI-labeled CHAMP peptides were present in discrete blue foci. To confirm that these foci represented CN peptide-containing integrins, we co-stained platelets with integrin-specific fluorescent monoclonal antibodies and found that CN peptide and antibody fluorescence coincided. Because 4CNI can readily be biosynthetically incorporated into proteins with little if any effect on protein structure and function, it provides a facile way to directly monitor protein behavior and protein−protein interactions in cellular environments. In addition, these results clearly demonstrate that the two-photon excitation cross section of 4CN-Trp is sufficiently large to make it a useful two-photon fluorescence reporter for biological applications.

Antibodies containing a fluorescent label or recombinant proteins containing a fluorescent reporter are essential tools for visualizing proteins and their interactions in situ.[1] However, antibodies and reporters can, by themselves, perturb protein structure and function.[2] An approach to overcoming this problem is to take advantage of the fluorescent properties of the natural amino acids tyrosine, phenylalanine, and tryptophan. Tryptophan is widely used for this purpose because its fluorescence has a relatively large quantum yield and it is sensitive to its environment, but tryptophan absorbs and emits in the ultraviolet (UV) region and has low photostability.[3] Accordingly, there has been substantial effort to modify tryptophan to improve its ability to function as a fluorescent reporter. For example, a series of azatryptophans have emission spectra red-shifted compared to those of tryptophan but have photophysical disadvantages that have

Received: April 2, 2021
Revised: May 7, 2021
Published: May 19, 2021

https://doi.org/10.1021/acs.biochem.1c00238
Biochemistry 2021, 60, 1722−1730

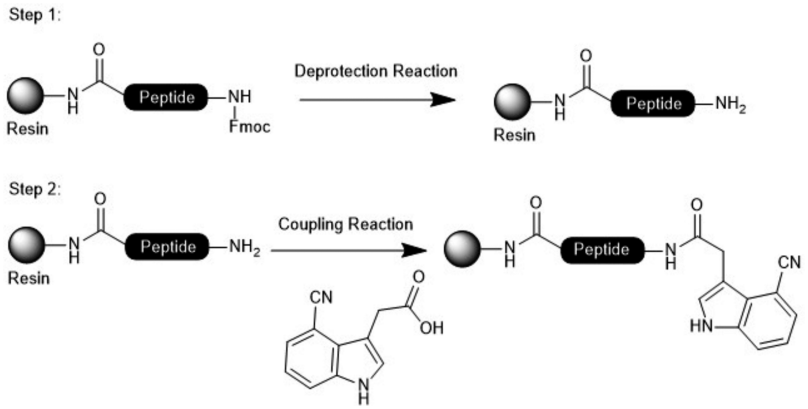

Figure 1. 4CNI-labeled antiplatelet integrin CHAMP peptides. CHAMP peptides were synthesized using an automated microwave peptide synthesizer and Fmoc-protected amino acids as described in Materials and Methods. After synthesis, the N-terminus of each peptide was capped and labeled with 4CNI-3AA. Labeled peptides were then cleaved from dried resin and purified by preparative scale RP-HPLC, and their masses analyzed using MALDI and electrospray ionization mass spectrometry. Reprinted with permission from ref 26. Copyright 2020 Elsevier. One or more co-authors of this paper are co-authors of the paper from which it is reprinted.

limited their application.[4−6] 6-Cyanotryptophan and 7-cyanotryptophan have increased quantum yields compared to that of tryptophan, but their emission maxima are at 370 and 390 nm, respectively, limiting their utility as visible fluorophores.[7] Recently, we discovered that 4-cyanotryptophan (4CN-Trp) and its side chain mimic 4-cyanoindole (4CNI) not only emit in the visible blue region (emission maximum at ∼420 nm) but also have unique photophysical properties: an absorption maximum at ∼325 nm, a large fluorescence quantum yield (>0.8 in aqueous solution), a long fluorescence lifetime (∼13 ns), and good photostability.[8] Taken together, these spectroscopic characteristics make 4CN-Trp (4CNI) a unique biological fluorescence reporter. Moreover, 4CNI-3-acetic acid (4CNI-3AA) is a commercially available mimic of 4CN-Trp that can be used to label the N-termini or lysines with 4CNI in a protein of interest, while tryptophan residues in polypeptide chains can be replaced with 4CN-Trp, as we have demonstrated.[9] In addition, 4CN-Trp can be prepared by a simple, high-yielding cost-effective synthetic route[10] or by biosynthesis in engineered microbes.[11] Because 4CN-Trp does not inhibit bacterial growth,[9] it is practical for cellular protein labeling applications.

The applicability of 4CN-Trp (4CNI) in one-photon fluorescence microscopy is well-established.[8,9,12] Here, we used 4CNI to image integrins on the surface of blood platelets by two-photon fluorescence microscopy, demonstrating the advantage of this fluorophore as an imaging agent. The particular advantages of using two-photon microscopy in conjunction with 4CNI labeling are the reduced phototoxicity by not exciting samples with UV light and the increased imaging depth, a clear advantage for three-dimensional and higher-resolution imaging. In this study, we appended 4CNI to the amino termini of CHAMP (computed helical anti-membrane protein) peptides that spontaneously insert into cellular lipid bilayers and target the transmembrane (TM) domains of integrins in a sequence-specific manner.[13]

Importantly, CHAMP peptides also induce integrin activation, promoting the binding of integrin to extracellular ligands by causing separation of the TM domain heterodimers that maintain integrins in their inactive states. We found that 4CNI labeling did not perturb the ability of the CHAMP peptides to cause integrin activation. Thus, 4CNI-labeled anti-αIIb TM caused αIIbβ3-dependent platelet aggregation, 4CNI-labeled anti-αv TM caused the $\alpha v\beta 3$-dependent adhesion of CHO cells to osteopontin (OPN), and 4CNI-labeled anti-β1 TM caused $\alpha 5\beta 1$-mediated platelet adhesion to fibronectin. In addition, using two-photon laser scanning deconvolution microscopy, we found that the 4CNI-labeled CHAMP peptides were present as a limited number of discrete blue clusters on the platelet surface that co-localized with fluorescently labeled integrin-specific monoclonal antibodies. Thus, these more detailed images confirm our previous observation that activating individual integrin molecules using CHAMP peptides can initiate integrin clustering in the absence of ligand binding.[14] The results also support previous evidence that the presence of 4CNI has little, if any, effect on protein structure and function. In addition, they show that 4CNI labeling, coupled with two-photon fluorescence microscopy, is a facile and biologically nontoxic way to monitor protein behavior and protein−protein interactions in cellular environments.

MATERIALS AND METHODS

Peptide Synthesis and Purification. CHAMP peptides (Figure 1 and Table 1) were synthesized using a Biotage Initiator+ Alstra automated microwave peptide synthesizer on preloaded ChemMatrix Rink-amide resin (Chem-Impex, 0.45 mmol/g) at a 0.1 mmol scale, as previously described.[15]

Table 1. 4CNI-Labeled CHAMP Peptides[a]

		ref
4CN-Trp*-anti-αIIb TM	X-KKAYVMLLPFFIGLLLGILFGGAFWGPARHLKK	13
4CN-Trp*-anti-αv TM	X-AYVFILLSFILGTLLGFLVMFWAKK	13
4CN-Trp*-anti-αIIbscr	X-KKAYVMLLGPFFILGLLIFFGAGWPARHGLKK	13
4CN-Trp*-anti-β1 TM	X-KKAWSLVLGGLIGSLIAFAVFLLLWKK	16

[a]X = 4CN indol ethyl amide. Amino acids are designated by their single-letter abbreviations.

https://doi.org/10.1021/acs.biochem.1c00238
Biochemistry 2021, 60, 1722−1730

Coupling of canonical Fmoc-protected amino acids to the resin was performed at 5 equiv premixed with 4.9 equiv of *O*-(1*H*-6-chlorobenzotriazol-1-yl)-1,1,3,3-tetramethyluronium hexafluorophosphate (HCTU, Chem-Impex) in the presence of 10 equiv of *N*,*N*-diisopropylethylamine (DIPEA, Sigma). Coupling was done once at 75 °C for 5 min for most amino acids and coupled twice for all β-branched amino acids. Standard Fmoc deprotection was performed twice at 70 °C for 5 min using 20% (v/v) 4-methylpiperidine (Sigma-Aldrich). After the polypeptide had been synthesized, the N-terminus was capped and labeled with 4CNI-3AA (Toronto Research Chemicals), where the coupling reaction was performed twice manually at room temperature for 1 h each using 2.5 equiv of 4CNI-3AA, 2.45 equiv of HCTU, and 10 equiv of DIPEA versus resin loading. Fmoc-protected amino acids were purchased from Chem-Impex.

Peptide cleavage was performed on dried resin using a TFA/TIPS/H_2O mixture (95:2.5:2.5) for 2 h at 22 °C; in the presence of Cys or Met, the cleavage cocktail was changed to a TFA/TIPS/H_2O/EDT mixture (92.5:2.5:2.5:2.5). The crude peptide mixture was then precipitated with cold diethyl ether. After being dried using N_2 gas, the crude peptide was dissolved in a 1:1 mixture of solvents A and B′ (solvent A, 0.1% TFA in H_2O; solvent B′, 0.1% TFA in 60% isopropanol, 30% CH_3CN, and 10% H_2O) and purified by preparative scale RP-HPLC using a C4 Vydac 214TP 300 Å 10 μm column (10 mm × 250 mm, Grace) with a flow rate of 5 mL/min over a linear gradient of 60% to 100% of buffer B′ over 40 min. The peptide mass was analyzed using MALDI (Shimadzu Axima) and electrospray ionization mass spectrometry (Qtrap 3200, ABSCI EX). The purity was determined by analytical HPLC using a C4 Jupiter 300 Å 10 μm column (4.6 mm × 30 mm, Phenomenex) and the same solvent system as for preparative HPLC. All peptide materials used for cellular studies were confirmed to be at least 95% pure. Organic solvents were purchased from Sigma-Aldrich.

Integrin Function Measurements. The effect of 4CNI labeling of the CHAMP peptide anti-αIIb TM on αIIbβ3-dependent platelet aggregation was measured using a Chrono-Log Model 700 Lumi-Aggregometer.[14] In studies approved by the Institutional Review Board of the University of Pennsylvania Office of Regulatory Affairs, human platelets, obtained from blood anticoagulated with 65 mM sodium citrate, 77 mM citric acid, and 95 mM glucose (pH 4.4), were washed with 10 mM HEPES buffer (pH 6.5) containing 150 mM NaCl, 3 mM EDTA, 1 μM PGE1, and 0.3 unit/mL apyrase and resuspended in modified Tyrode's buffer [20 mM HEPES (pH 7.35) containing 135 mM NaCl, 2.7 mM KCl, 3 mM NaH_2PO_4, and 5 mM glucose]. Aliquots (450 μL) of the washed platelets, supplemented with 200 μg/mL human fibrinogen and 1 mM $CaCl_2$, were stirred at 1200 rpm in siliconized aggregometer cuvettes. CHAMP peptides were dissolved in DMSO at final DMSO concentrations of ≤0.5%.

The effect of labeling anti-αv TM with 4CNI on the $\alpha v\beta 3$-dependent binding of OPN to CHO cells expressing human $\alpha v\beta 3$ was measured using an optical trap-based force spectroscopy method as previously described.[17] Briefly, a mixture of CHO cells and 2 μm OPN-coated carboxylate-modified latex beads (~10^6 mL^{-1} each) (Bangs Laboratories) suspended in a culture medium was placed in a flow chamber. After the CHO cells were allowed to settle onto the polylysine-coated bottom of the chamber, an OPN-coated bead was trapped by the focused laser beam, oscillated in the *X*-direction in a triangular waveform at a frequency of 10 Hz and at constant peak-to-peak amplitude of 0.8 μm, and brought into repeated contact with an adherent CHO cell by micromanipulation using a keyboard-governed piezoelectric stage. Data collection was initiated at first contact between the bead and cell, and the force exerted by the trap to separate the bead and cell was recorded in each oscillation cycle. Data were analyzed with custom LabVIEW (National Instruments, Austin, TX) software. Rupture forces were sorted into a histogram with 5 pN-wide bins and normalized by the total number of contacts. The percentage of events in a particular force range (bin) represented the probability of rupture events at that tension. To preclude the inclusion of nonspecific surface interactions of CHO cells in the data analysis, the cumulative binding probability of forces of >60 pN was used as a quantitative measure of specific $\alpha v\beta 3$ ligand binding activity.[18]

To determine if appending 4CNI to the N-terminus of anti-β1 TM CHAMP perturbs its ability to enhance fibronectin binding to $\alpha 5\beta 1$, we used a solid-phase assay in which 3×10^5 washed human platelets suspended in Tyrode's buffer containing 0.1 mM eptifibatide were added to the wells of Immulon 2HB flat bottom microtiter plates (Thermo Scientific) coated previously with 5 mg/mL bovine serum albumin (BSA) (Fisher Scientific) or 20 μg/mL fibronectin (Sigma-Aldrich). The plates were then incubated for 30 min at 37 °C before being washed three times with PBS. The number of adherent platelets was enumerated using a colorimetric assay for platelet peroxidase activity;[19] 150 μL aliquots of 0.1 M sodium citrate (pH 5.4) containing 0.1% Triton X-100 and 4 mM *p*-nitrophenyl phosphate were added to the wells. After a 30 min incubation at 37 °C in the dark, 100 μL of 2 N NaOH was added to the wells to stop the reaction and the absorbance was measured at 405 nm using an Accuris Instruments Smartreader plate reader. As a positive control, platelet suspensions were preincubated with 1 mM $MnCl_2$; as a negative control, platelet suspensions were incubated without stimulation. Specific binding was assessed by preincubating the platelet suspensions with 4 mM EDTA to suppress platelet adhesion.

Confocal Fluorescence Imaging via Two-Photon Excitation and Deconvolution Fluorescence Microscopy. To visualize αIIbβ3, $\alpha v\beta 3$, and $\alpha 5\beta 1$ on the platelet surface, we resuspended washed human platelets at a concentration of 2.5×10^8 platelets/mL in modified Tyrode's buffer without BSA. Aliquots (500 μL) of the platelet suspension were transferred to BSA-blocked centrifuge tubes and incubated for 60 s at 37 °C in the presence or absence of 2 μM 4CNI-labeled anti-αIIb TM, anti-αIIbscr, anti-αv TM, or anti-β1 TM. The platelets were then transferred to poly-L-lysine-coated glass coverslips and allowed to settle on the coverslips at room temperature. After 30 min, the coverslips were washed in PBS, blocked with 5% BSA for 30 min at room temperature, washed again with PBS, and incubated with the corresponding Alexa Fluor 568-conjugated anti-β3 monoclonal antibody SSA6, anti-$\alpha v\beta 3$ monoclonal antibody 23C6 (R&D Systems), or anti-β1 monoclonal antibody P5D2 (R&D Systems) for 1 h at 37 °C. After platelets that adhered to the coverslips were fixed with 4% paraformaldehyde, the coverslips were mounted on glass slides using Fluoromount G (Southern Biotech) and transported to the Penn Vet Imaging Core Facility where they were imaged using a Leica SP8 laser scanning confocal/multiphoton microscope and a 100× (1.46

https://doi.org/10.1021/acs.biochem.1c00238
Biochemistry 2021, 60, 1722−1730

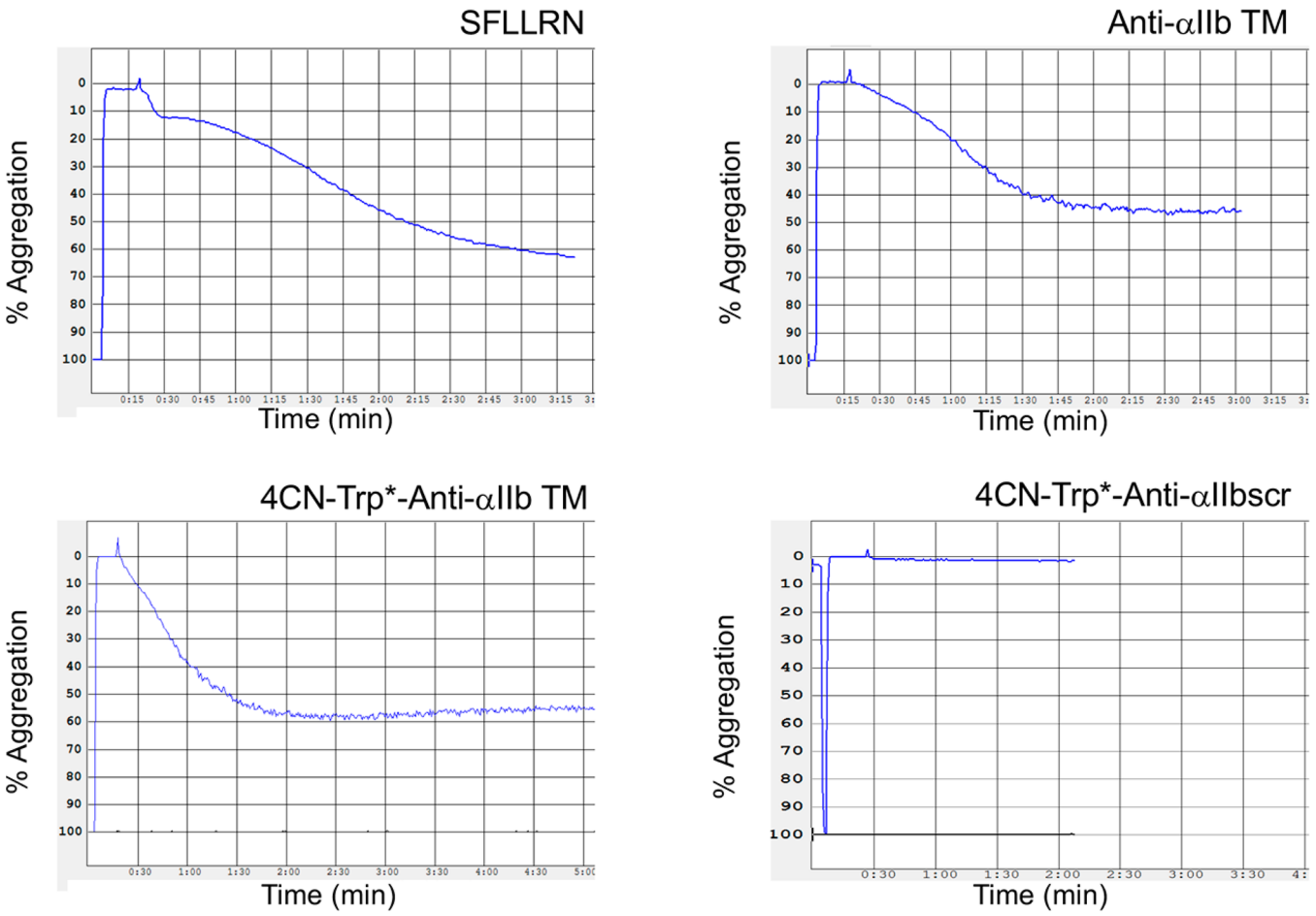

Figure 2. 4CNI-labeled CHAMP peptide 4CN-Trp*-anti-αIIb TM causes platelet aggregation. Comparison of the extent of turbidometric platelet aggregation stimulated by platelet thrombin receptor activation peptide SFLLRN (50 μM), CHAMP peptide anti-αIIb TM (2 μM), 4CNI-labeled CHAMP peptide 4CN-Trp*-anti-αIIb (2 μM), and 4CNI-labeled scrambled peptide 4CN-Trp*-anti-αIIbscr TM (2 μM).

NA) oil-immersion lens with an additional optical zoom of 5×. Images were taken with a sequential scan. The first scan for Alexa Fluor 568 red fluorescence was taken with the confocal laser at a power of 5% and an excitation wavelength of 552 nm. Acquisition was performed with the internal HyD detector over the emission range of 569−628 nm. The second scan for CNI blue fluorescence was taken with the two-photon laser tuned to 694 nm at 25% transmission (90% gain). Acquisition was performed with the internal HyD detector over the emission range of 390−448 nm. The images were then subjected to deconvolution processing using Huygens Essential Software, version 17.04.1p2 64b (Hilversum, The Netherlands).

RESULTS

Previously, we detected αIIbβ3 clusters on platelets that had been incubated with the CHAMP peptide anti-αIIb TM, fixed with paraformaldehyde, and then stained with a fluorescently labeled anti-β3 monoclonal antibody.[14] However, to more directly visualize CHAMP peptide-induced αIIbβ3 clusters, as well as clusters of other platelet integrins, we took advantage of the observation that proteins labeled with 4CNI exhibit visible blue fluorescence.[8] Accordingly, we synthesized membrane-soluble ∼25−28-residue anti-αIIb, anti-αv, and anti-β1 TM domain CHAMP peptides that were each labeled with 4CNI-3AA at their N-termini (4CN-Trp*-anti-αIIb TM, 4CN-Trp*-anti-αv TM, and 4CN-Trp*-anti-β1 TM) as previously described (Table 1).[8]

CHAMP peptides assume a nearly vertical α-helical transmembrane orientation in membrane bilayers, enabling them to interact with their designated targets.[20] To confirm that appending 4CNI to the N-termini of the various CHAMP peptides does not perturb their interaction with membranes and their subsequent ability to cause integrin activation, we incubated washed human platelets with 4CN-Trp*-anti-αIIb TM, transfected CHO cells with 4CN-Trp*-anti-αv TM, and washed human platelets with 4CN-Trp*-anti-β1 TM and measured the effect on αIIbβ3, αvβ3, and α5β1 function, respectively.

Shifting αIIbβ3 on platelets from its inactive to its active conformation is required for platelet aggregation.[13] We found that like the thrombin receptor-activating peptide SFLLRN at 50 μM and the unmodified CHAMP peptide anti-αIIb TM, 2 μM 4CN-Trp*-anti-αIIb TM caused αIIbβ3-dependent platelet aggregation, whereas a 33-residue 4CNI-labeled scrambled peptide at the same concentration had no effect (Figure 2). Thus, these results indicate that despite the presence of 4CNI at its N-terminus, 4CN-Trp*-anti-αIIb TM retains the ability to cause αIIbβ3 activation.

Next, to verify that appending 4CNI to anti-αv TM does not perturb its ability to activate αvβ3, we used optical trap-based force spectroscopy to measure the interaction of matrix protein

https://doi.org/10.1021/acs.biochem.1c00238
Biochemistry 2021, 60, 1722−1730

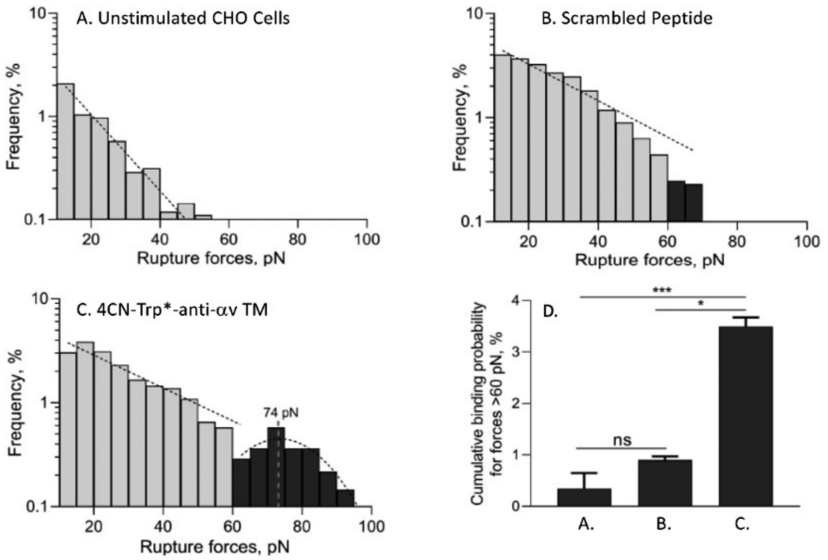

Figure 3. Effect of 4CNI-labeled CHAMP peptides on the binding of osteopontin (OPN) to $\alpha v\beta 3$. The binding of OPN to human $\alpha v\beta 3$ expressed by CHO cells was measured using optical trap-based force spectroscopy as described in Materials and Methods. The histograms shown in the figure represent the distribution of rupture forces between $\alpha v\beta 3$-expressing CHO cells and OPN-coated latex beads trapped and oscillated by the focused laser beam. (A) Untreated CHO cells expressing human $\alpha v\beta 3$ (12338 rupture events). (B) CHO cells expressing $\alpha v\beta 3$ incubated with 5 μM 4CNI-labeled scrambled CHAMP peptide for 15 min (10817 rupture events). (C) CHO cells expressing $\alpha v\beta 3$ incubated with 5 μM 4CN-Trp*-anti-αv TM for 15 min (11013 rupture events). The dashed lines show best-fit analyses using an exponential function for <60 pN nonspecific interactions and a Gaussian function for specific >60 pN $\alpha v\beta 3$−OPN interactions. The best-fit parameters for the exponential function $a \times \exp(bF)$ were (A) 5.70 ± 0.58; −0.085 ± 0.006, (B) 7.32 ± 0.67; −0.040 ± 0.003, and (C) 5.97 ± 0.80; −0.037 ± 0.005. Best-fit coefficients for the Gaussian function in panel C: $A \exp\left(-0.5\frac{F-F_m}{SD}^2\right)$. A = 0.45 ± 0.05. F_m = 73.56 ± 2.05. SD = 12.99 ± 2.26. (D) Statistical analysis of the cumulative binding probability for the specific interactions between $\alpha v\beta 3$ and OPN as reflected by >60 pN rupture forces. (A) Unstimulated CHO cells. (B) Scrambled peptide. (C) 4CN-Trp*-anti-αv TM: ns, not significant; *$p < 0.05$; ***$p < 0.001$ (Kruskal−Wallis test with Dunn's post hoc test).

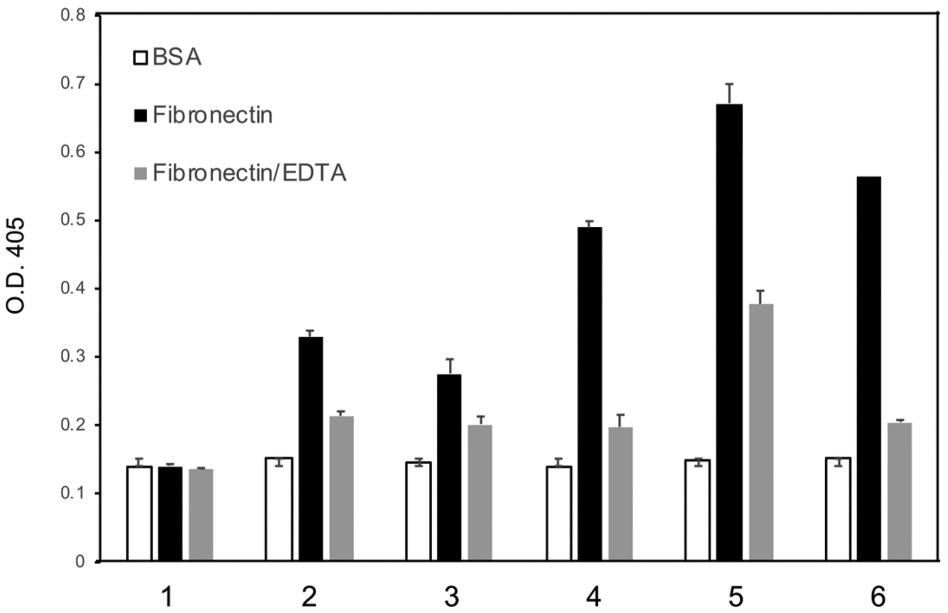

Figure 4. 4CNI-labeled CHAMP peptide 4CN-Trp*-anti-$\beta 1$ TM stimulates adhesion of platelets to fibronectin. The adhesion of washed human platelets to the wells of microtiter plates coated with either BSA (white bars) or fibronectin (black bars) was measured as described in Materials and Methods. As a positive control, platelets were preincubated with 1 mM $MnCl_2$; unstimulated platelets served as a negative control. Specific platelet adhesion to fibronectin was adhesion inhibited by preincubating the platelets with 4 mM EDTA (gray bars). The data shown are the mean and one standard deviation of measurements made in triplicate and are representative of five separate experiments: (1) colorimetric assay performed in the absence of platelets, (2) unstimulated platelets, (3) 2 μM 4CN-Trp*-anti-αIIbscr, (4) 1 mM $MnCl_2$, (5) 2 μM anti-$\beta 1$ TM, and (6) 2 μM 4CN-Trp*-anti-$\beta 1$ TM.

OPN with single $\alpha v\beta 3$ molecules on CHO cells expressing human $\alpha v\beta 3$.[17] As shown by the histograms in Figure 3, compared to unstimulated CHO cells (Figure 3A) or cells incubated with the scrambled peptide (Figure 3B), incubating

https://doi.org/10.1021/acs.biochem.1c00238
Biochemistry 2021, 60, 1722−1730

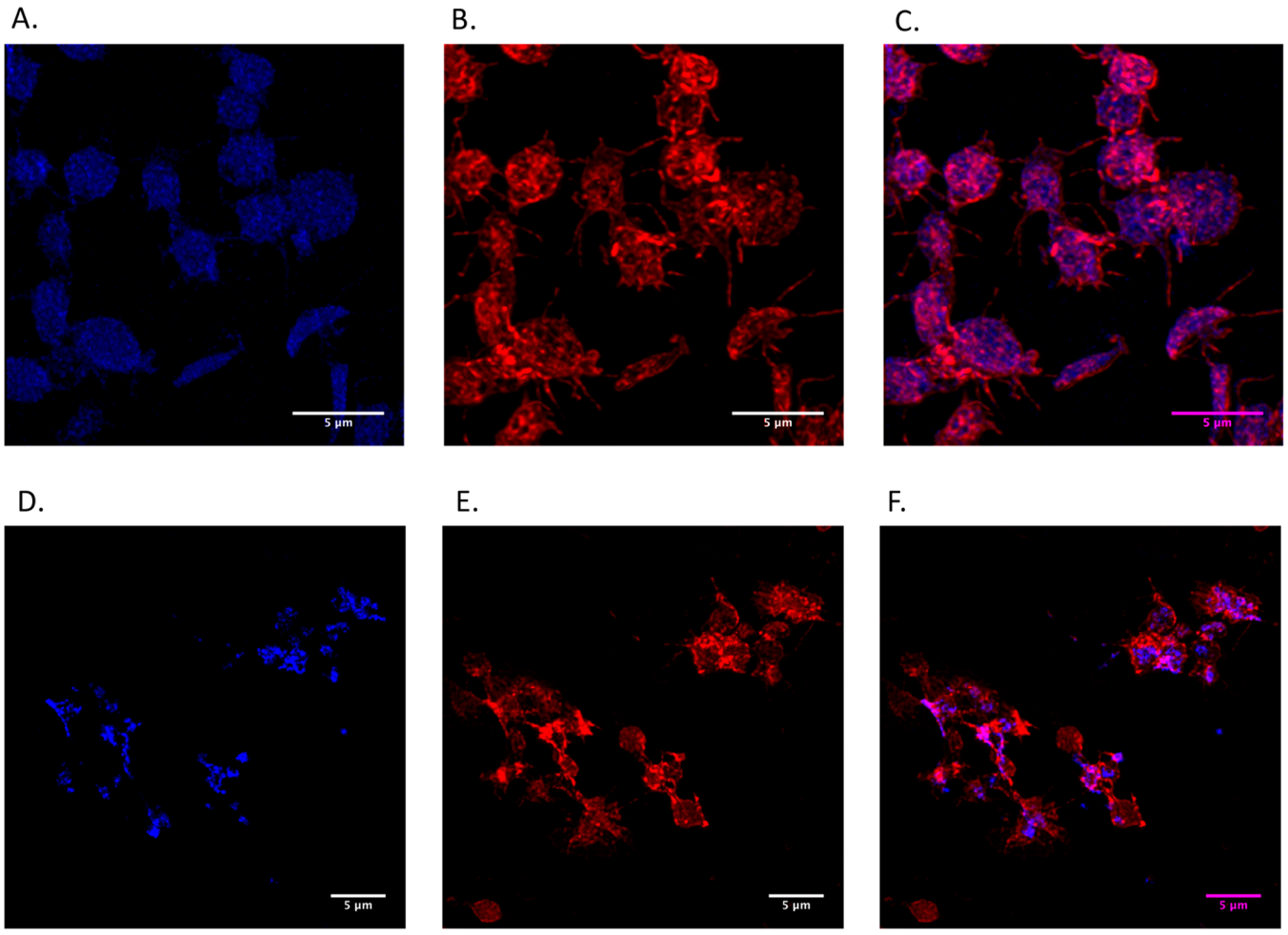

Figure 5. Two-photon deconvolution fluorescence microscopy imaging of 4CN-Trp*-anti-αIIb TM bound to αIIbβ3 on the platelet surface. (A) Washed human platelets incubated with the CNI-labeled scrambled peptide 4CN-Trp*-anti-αIIbscr for 60 s. (B) Platelets from panel A stained with Alexa Fluor 568-conjugated anti-β3 monoclonal antibody SSA6. (C) Merge of the images from panels A and B. (D) Washed human platelets incubated with the CNI-labeled peptide 4CN-Trp*-anti-αIIb TM for 60 s. (E) Platelets from panel D stained with Alexa Fluor 568-conjugated anti-β3 monoclonal antibody SSA6. (F) Merged image of panels D and E.

CHO cells with 4CN-Trp*-anti-αv TM resulted in an ≈7-fold increase in the cumulative probability of specific αvβ3−OPN binding (Figure 3C). The effect of 4CN-Trp*-anti-αv TM was a consequence of its specific interaction with αv because rupture forces of >60 pN, previously shown to be specific for binding of OPN to αvβ3,[17] were present only as a distinct force peak when the CHO cells were incubated with 4CN-Trp*-anti-αv TM, but not with the scrambled peptide. A statistical analysis of these results is shown in Figure 3D.

Platelets express three fibronectin-binding integrins (αIIbβ3, αvβ3, and α5β1) whose ability to interact with fibronectin is regulated by cellular agonists and divalent cations.[21] We recently designed a CHAMP peptide, designated anti-β1 TM, that binds tightly to the β1 TM domain.[16] To determine if anti-β1 TM increases platelet α5β1 ligand binding activity, we used a solid-phase assay to measure the adherence of platelets to the wells of microtiter plates coated with human fibronectin. Because the interaction of α5β1 with fibronectin is dependent on the presence of divalent cations,[21] we defined specific adherence as adherence that was inhibited by chelating divalent cations using EDTA. In the absence of agonist stimulation, there was a 2.5-fold increase in the number of adherent platelets when the microtiter plate wells were coated with fibronectin rather than bovine serum albumin, indicating a level of constitutive α5β1-mediated fibronectin binding activity that was unchanged when the platelets were preincubated with the scrambled CHAMP peptide (Figure 4). Adherence increased an additional 2.5-fold over baseline when the platelets were preincubated with 1 mM Mn^{2+}, an increase comparable to that seen upon preincubation of the platelets with 2 μM CHAMP peptide anti-β1 TM. In addition, we found that appending 4CNI to the N-terminus of anti-β1 TM (CN-Trp*-anti-β1 TM) did not perturb the ability of the CHAMP peptide to enhance the adhesion of platelets to fibronectin and appeared to work at least as well as the native CHAMP.

Having demonstrated that appending 4CNI to the N-termini of CHAMP peptides does not impair their ability to induce platelet integrin function, we used two-photon deconvolution fluorescence microscopy to image 4CNI-containing integrins on the platelet surface. As shown in Figure 5A−C, both the 4CNI-modified scrambled control peptide anti-αIIbscr and the Alexa Fluor 568-labeled anti-β3 monoclonal antibody SSA6 uniformly decorated the platelet cell surface. By contrast, incubating platelets with 2 μM 4CN-Trp*-anti-αIIb TM for 60 s caused the distribution of αIIbβ3 into discrete blue nodular

https://doi.org/10.1021/acs.biochem.1c00238
Biochemistry 2021, 60, 1722−1730

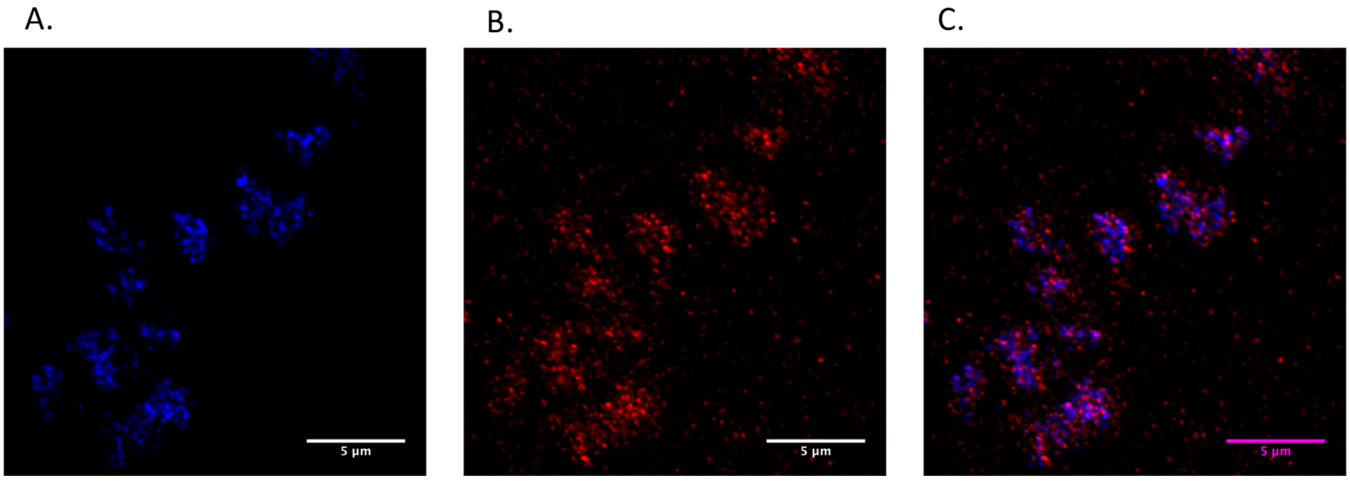

Figure 6. Two-photon deconvolution fluorescence microscopy imaging of 4CN-Trp*-anti-αv TM bound to $\alpha v\beta 3$ on the platelet surface. (A) Washed human platelets incubated with the CNI-labeled peptide 4CN-Trp*-anti-αv TM for 60 s. (B) Platelets from panel A stained with Alexa Fluor 568-conjugated $\alpha v\beta 3$ monoclonal antibody 23C6. (C) Merged image of panels A and B.

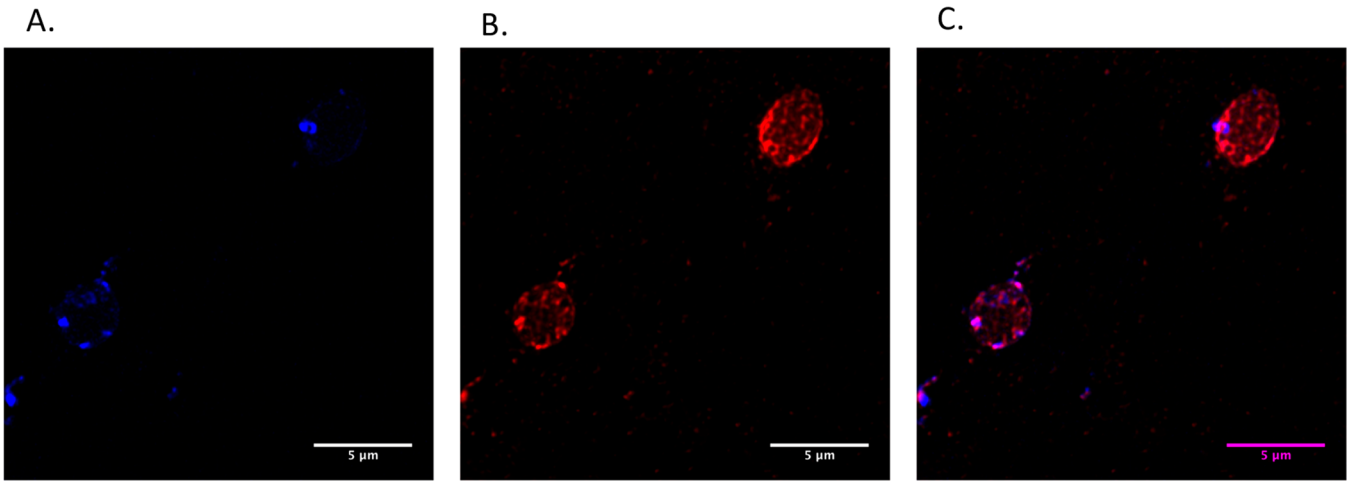

Figure 7. Two-photon deconvolution fluorescence microscopy imaging of 4CN-Trp*-anti-β1 TM bound to $\alpha 5\beta 1$ on the platelet surface. (A) Washed human platelets incubated with the CNI-labeled peptide 4CN-Trp*-anti-β1 TM for 60 s. (B) Platelets from panel A stained with Alexa Fluor 568-conjugated anti-β1 monoclonal antibody P5D2. (C) Merged image of panels A and B.

densities whose distribution coincided with that of Alexa Fluor 568-labeled SSA6 (Figure 5D−F). This result is consistent with our previous observation that incubating platelets with an anti-αIIb TM CHAMP results in the formation of $\alpha IIb\beta 3$ clusters.[14] However, by labeling anti-αIIb TM with 4CNI, we were able, for the first time, to image $\alpha IIb\beta 3$ clusters without the need to first fix the cells to preclude antibody-induced clustering.

Although the αv and αIIb TM domains are highly similar, the CHAMP peptides anti-αv TM and anti-αIIb TM exclusively bind to their cognate TM domains and specifically activate the respective integrins.[13] However, there are substantially more copies of $\alpha IIb\beta 3$ per platelet than $\alpha v\beta 3$.[19] Therefore, to determine if 4CN-Trp*-anti-αv TM is sufficiently sensitive to image platelet $\alpha v\beta 3$, we incubated platelets with 4CN-Trp*-anti-αv TM and imaged the platelets by two-photon deconvolution fluorescence microscopy. As shown in Figure 6, 2 μM 4CN-Trp*-anti-αv TM was present in blue nodular densities on the platelet surface whose distribution mirrored that of $\alpha v\beta 3$ monoclonal antibody 23C6. Because of the decreased number of $\alpha v\beta 3$ molecules per platelet compared to $\alpha IIb\beta 3$, the size and intensity of the 4CN-Trp*-anti-αv TM-labeled clusters were decreased compared to the values of those labeled with 4CN-Trp*-anti-αIIb TM. Nonetheless, these images indicate that like CHAMP peptide-induced $\alpha IIb\beta 3$ clustering, binding of the CHAMP peptide to the αv TM domain caused $\alpha v\beta 3$ clustering.

It has been estimated that platelets express 2000−4000 copies of $\alpha 5\beta 1$ per platelet,[22] substantially fewer than the number of $\alpha IIb\beta 3$ molecules.[23] To image activated platelet $\alpha 5\beta 1$, we incubated resting platelets with 2 μM 4CN-Trp*-anti-β1 TM for 60 s and then used two-photon deconvolution fluorescence microscopy to image the platelet surface. As shown in Figure 7, 4CN-Trp*-anti-β1 TM was present as a small number of blue nodules on the platelet surface whose distribution coincided with that of anti-α5 monoclonal antibody P5D2. Thus, like the 4CNI-labeled anti-αIIb TM and anti-αv TM CHAMP peptides, binding of 4CN-Trp*-anti-β1 TM to the α5 TM causes $\alpha 5\beta 1$ clustering.

https://doi.org/10.1021/acs.biochem.1c00238
Biochemistry 2021, 60, 1722−1730

DISCUSSION

4-Cyanotryptophan is a minimally perturbing blue fluorescent unnatural amino acid analogue with unique photophysical properties that can be incorporated biosynthetically into proteins.[8] The N-termini of proteins and peptides can also be readily labeled with 4CN using 4CNI-3AA, which is available commercially.[12] Previously, we appended 4CNI to the amino terminus of the antimicrobial peptide Mastoparan X and used wide-field fluorescence microscopy to demonstrate binding of the peptide to the cell membrane of HEK293/T17 cells and permeation of the peptide into the cytosol.[8] Using confocal microscopy, we were also able to show that Mastoparan X caused HEK cell death by apoptosis rather than necrosis. Similarly, using wide-field fluorescence microscopy, we demonstrated that an exogenous 4CN-labeled peptide derived from the HIV protein REV was taken up by and concentrated in the nuclei of HeLa cells.[12] We also used microwave-assisted solid-phase peptide synthesis to replace Trp9 of the model peptide pHLIP [pH-(low) insertion peptide] with 4CNTrp and again used wide-field fluorescence microscopy to show that 4CNTrp-labeled pHLIP retained the ability to bind to HeLa cell membranes in a pH-dependent manner.[9]

To further demonstrate the utility of 4CNI as an imaging agent, we employed it here to visualize integrins on the surface of blood platelets by two-photon fluorescence microscopy. In comparison to one-photon excitation (1PE), two-photon excitation (2PE) offers several advantages, including higher spatial resolution, deeper penetration, less photobleaching, and less phototoxicity.[24] In addition, the absorption spectrum of 4CNI can be readily accessed by the femtosecond Ti:sapphire laser commonly equipped in commercial 2PE microscopes. Confirming the utility of 4CNI in 2PE fluorescence microscopy will open up new biological applications for this amino acid fluorophore and its nucleic acid analogue, 4-cyanoindole 2′-deoxyribonucleoside.[25]

We used 4CNI-3AA to label the N-termini of membrane-soluble CHAMP peptides designed to specifically bind to integrin transmembrane domains in situ. Because these peptides bind to one component of the transmembrane heterodimer that maintains integrins in their inactive conformation, they cause heterodimer separation and subsequent integrin activation.[13] Previously, we used wide-field fluorescence microscopy of platelets stained with an Alexa Fluor-labeled anti-β3 monoclonal antibody to show that in addition to causing αIIbβ3 activation, the CHAMP peptide anti-αIIb TM also causes the formation of αIIbβ3 clusters.[14] However, because antibodies are bivalent, it was necessary to fix the platelets with paraformaldehyde before antibody staining to preclude the possibility that the antibody, rather than anti-αIIb TM, caused αIIbβ3 clustering. The advantage of appending a small nonperturbing 4CN label to the N-termini of CHAMP peptides is that it enabled us to visualize the formation of integrin clusters on the surface of living platelets and at the high resolution of two-photon laser scanning fluorescence microscopy. Thus, we found that compared to a 4CNI-labeled scrambled peptide that uniformly decorates the platelet surface, the CNI-labeled CHAMP peptides were present in a limited number of discrete foci that co-localize with Alexa Fluor 568-labeled integrin-specific monoclonal antibodies, confirming the ability of the CNI-labeled peptides to image integrins embedded in cell membranes. In addition, CNI labeling did not impair the functional effects of the CHAMP peptides. Because 4CNI can readily be biosynthetically incorporated into proteins with little if any effect on protein structure and function, it provides a facile way to directly monitor protein behavior and protein−protein interactions in cellular environments. Finally, our imaging results clearly demonstrated that the 2PE cross section of 4CN-Trp is sufficiently large (at 694 nm), making it a useful two-photon fluorescence reporter for biological applications, although additional cases will certainly be required to confirm the generality of our results. As the 2PE energy used in this study is located at the tail region of the one-photon absorption spectrum of 4CN-Trp, it is expected that its 2PE brightness will further increase when a shorter 2PE wavelength is used.

AUTHOR INFORMATION

Corresponding Author

Joel S. Bennett − *Hematology-Oncology Division, Department of Medicine, Perelman School of Medicine, University of Pennsylvania, Philadelphia, Pennsylvania 19104, United States;* orcid.org/0000-0003-4650-221X; Phone: 610-506-8937; Email: bennetts@pennmedicince.upenn.edu

Authors

Karen P. Fong − *Hematology-Oncology Division, Department of Medicine, Perelman School of Medicine, University of Pennsylvania, Philadelphia, Pennsylvania 19104, United States*

Ismail A. Ahmed − *Department of Biochemistry and Biophysics, University of Pennsylvania, Philadelphia, Pennsylvania 19104, United States*

Marco Mravic − *Department of Pharmaceutical Chemistry, University of California, San Francisco, San Francisco, California 94158-2517, United States*

Hyunil Jo − *Department of Pharmaceutical Chemistry, University of California, San Francisco, San Francisco, California 94158-2517, United States;* orcid.org/0000-0002-4863-0779

Oleg V. Kim − *Department of Cell and Developmental Biology, Perelman School of Medicine, University of Pennsylvania, Philadelphia, Pennsylvania 19104, United States*

Rustem I. Litvinov − *Department of Cell and Developmental Biology, Perelman School of Medicine, University of Pennsylvania, Philadelphia, Pennsylvania 19104, United States*

John W. Weisel − *Department of Cell and Developmental Biology, Perelman School of Medicine, University of Pennsylvania, Philadelphia, Pennsylvania 19104, United States*

William F. DeGrado − *Department of Pharmaceutical Chemistry, University of California, San Francisco, San Francisco, California 94158-2517, United States*

Feng Gai − *Department of Chemistry, University of Pennsylvania, Philadelphia, Pennsylvania 19104-6323, United States;* orcid.org/0000-0003-1621-7119

Complete contact information is available at: https://pubs.acs.org/10.1021/acs.biochem.1c00238

Funding

This work was supported by National Institutes of Health Grants R35GM122603 (to W.F.D.) and HL146373 (to J.S.B., J.W.W., and W.F.D.). F.G. acknowledges the Research

Foundation of the University of Pennsylvania for support. I.A.A. is supported by a NINDS D-SPAN Fellowship (F99 NS108544-01). M.M. is supported by an HHMI Gilliam Fellowship. R.I.L. acknowledges the Program for Competitive Growth at Kazan Federal University. O.V.K. is supported by American Heart Association Grant 17SDG33680177.

Notes

The authors declare no competing financial interest.

■ ACKNOWLEDGMENTS

The authors acknowledge National Institutes of Health Grant S10OD021633 awarded to Bruce D. Freedman for acquisition of instrumentation utilized in the Penn Vet Imaging Core facility.

■ REFERENCES

(1) Shaner, N. C., Steinbach, P. A., and Tsien, R. Y. (2005) A guide to choosing fluorescent proteins. *Nat. Methods 2*, 905−909.
(2) Gosavi, P. M., and Korendovych, I. V. (2016) Minimalist IR and fluorescence probes of protein function. *Curr. Opin. Chem. Biol. 34*, 103−109.
(3) Royer, C. A. (2006) Probing protein folding and conformational transitions with fluorescence. *Chem. Rev. 106*, 1769−1784.
(4) Smirnov, A. V., English, D. S., Rich, R. L., Lane, J., Teyton, L., Schwabacher, A. W., Luo, S., Thornburg, R. W., and Petrich, J. W. (1997) Photophysics and biological applications of 7-azaindole and its analogs. *J. Phys. Chem. B 101*, 2758−2769.
(5) Lepthien, S., Hoesl, M. G., Merkel, L., and Budisa, N. (2008) Azatryptophans endow proteins with intrinsic blue fluorescence. *Proc. Natl. Acad. Sci. U. S. A. 105*, 16095−16100.
(6) Talukder, P., Chen, S., Liu, C. T., Baldwin, E. A., Benkovic, S. J., and Hecht, S. M. (2014) Tryptophan-based fluorophores for studying protein conformational changes. *Bioorg. Med. Chem. 22*, 5924−5934.
(7) Talukder, P., Chen, S., Roy, B., Yakovchuk, P., Spiering, M. M., Alam, M. P., Madathil, M. M., Bhattacharya, C., Benkovic, S. J., and Hecht, S. M. (2015) Cyanotryptophans as Novel Fluorescent Probes for Studying Protein Conformational Changes and DNA-Protein Interaction. *Biochemistry 54*, 7457−7469.
(8) Hilaire, M. R., Ahmed, I. A., Lin, C. W., Jo, H., DeGrado, W. F., and Gai, F. (2017) Blue fluorescent amino acid for biological spectroscopy and microscopy. *Proc. Natl. Acad. Sci. U. S. A. 114*, 6005−6009.
(9) Zhang, K., Ahmed, I. A., Kratochvil, H. T., DeGrado, W. F., Gai, F., and Jo, H. (2019) Synthesis and application of the blue fluorescent amino acid l-4-cyanotryptophan to assess peptide-membrane interactions. *Chem. Commun. (Cambridge, U. K.) 55*, 5095−5098.
(10) Micikas, R., Acharyya, A., Gai, F., and Smith, A. B., 3rd. (2021) A Scalable Synthesis of the Blue Fluorescent Amino Acid 4-Cyanotryptophan and the Fmoc Derivative: Utility Demonstrated with the Influenza M2 Peptide Tetramer. *Org. Lett. 23*, 1247−1250.
(11) Boville, C. E., Romney, D. K., Almhjell, P. J., Sieben, M., and Arnold, F. H. (2018) Improved Synthesis of 4-Cyanotryptophan and Other Tryptophan Analogues in Aqueous Solvent Using Variants of TrpB from Thermotoga maritima. *J. Org. Chem. 83*, 7447−7452.
(12) Ahmed, I. A., Rodgers, J. M., Eng, C., Troxler, T., and Gai, F. (2019) PET and FRET utility of an amino acid pair: tryptophan and 4-cyanotryptophan. *Phys. Chem. Chem. Phys. 21*, 12843−12849.
(13) Yin, H., Slusky, J. S., Berger, B. W., Walters, R. S., Vilaire, G., Litvinov, R. I., Lear, J. D., Caputo, G. A., Bennett, J. S., and DeGrado, W. F. (2007) Computational design of peptides that target transmembrane helices. *Science 315*, 1817−1822.
(14) Fong, K. P., Zhu, H., Span, L. M., Moore, D. T., Yoon, K., Tamura, R., Yin, H., DeGrado, W. F., and Bennett, J. S. (2016) Directly Activating the Integrin alphaIIbbeta3 Initiates Outside-In Signaling by Causing alphaIIbbeta3 Clustering. *J. Biol. Chem. 291*, 11706−11716.
(15) Mravic, M., Thomaston, J. L., Tucker, M., Solomon, P. E., Liu, L., and DeGrado, W. F. (2019) Packing of apolar side chains enables accurate design of highly stable membrane proteins. *Science 363*, 1418−1423.
(16) Mravic, M., Hu, H., Lu, Z., Bennett, J. S., Sanders, C. R., Orr, A. W., and DeGrado, W. F. (2018) De novo designed transmembrane peptides activating the alpha5beta1 integrin. *Protein Eng., Des. Sel. 31*, 181−190.
(17) Litvinov, R. I., Vilaire, G., Shuman, H., Bennett, J. S., and Weisel, J. W. (2003) Quantitative analysis of platelet alpha v beta 3 binding to osteopontin using laser tweezers. *J. Biol. Chem. 278*, 51285−51290.
(18) Litvinov, R. I., Vilaire, G., Li, W., DeGrado, W. F., Weisel, J. W., and Bennett, J. S. (2006) Activation of individual alphaIIbbeta3 integrin molecules by disruption of transmembrane domain interactions in the absence of clustering. *Biochemistry 45*, 4957−4964.
(19) Bennett, J. S., Chan, C., Vilaire, G., Mousa, S. A., and DeGrado, W. F. (1997) Agonist-activated avb3 on platelets and lymphocytes binds to the matrix protein osteopontin. *J. Biol. Chem. 272*, 8137−8140.
(20) Caputo, G. A., Litvinov, R. I., Li, W., Bennett, J. S., Degrado, W. F., and Yin, H. (2008) Computationally designed peptide inhibitors of protein-protein interactions in membranes. *Biochemistry 47*, 8600−8606.
(21) Gailit, J., and Ruoslahti, E. (1988) Regulation of the fibronectin receptor affinity by divalent cations. *J. Biol. Chem. 263*, 12927−12932.
(22) Ni, H., and Freedman, J. (2003) Platelets in hemostasis and thrombosis: role of integrins and their ligands. *Transfus Apher Sci. 28*, 257−264.
(23) Bennett, J. S. (2005) Structure and function of the platelet integrin alphaIIbbeta3. *J. Clin. Invest. 115*, 3363−3369.
(24) Helmchen, F., and Denk, W. (2005) Deep tissue two-photon microscopy. *Nat. Methods 2*, 932−940.
(25) Ahmed, I. A., Acharyya, A., Eng, C. M., Rodgers, J. M., DeGrado, W. F., Jo, H., and Gai, F. (2019) 4-Cyanoindole-2′-deoxyribonucleoside as a Dual Fluorescence and Infrared Probe of DNA Structure and Dynamics. *Molecules 24* (3), 602.
(26) Acharyya, A., Ahmed, I. A., and Gai, F. (2020) 4-Cyanoindole-based fluorophores for biological spectroscopy and microscopy. *Methods Enzymol. 639*, 191−215.

https://doi.org/10.1021/acs.biochem.1c00238
Biochemistry 2021, 60, 1722−1730